

Quark model of the $\pi^- pp \rightarrow pn$ reaction

Gerald A. Miller

Institute for Nuclear Theory, Department of Physics, University of Washington, Seattle, Washington 98195

Avraham Gal

Racah Institute of Physics, The Hebrew University, Jerusalem 91904, Israel

(Received 4 February 1987; revised manuscript received 15 September 1987)

A model employing quark dynamics is applied to the $\pi^- + pp \rightarrow pn$ reaction. Quark effects can provide a substantial contribution to the total absorption cross section, and qualitatively reproduce the measured angular distributions.

I. INTRODUCTION

A pion can lose all of its energy and excite various final states containing no real pion in its interaction with a nucleus. Such a process is called a pion absorption reaction. Understanding pion absorption requires knowledge of some of the best kept secrets of nuclear dynamics: the short ranged part of the baryon-baryon interaction. One important question is whether quark degrees of freedom are required. The dependence on small separations arises because pion absorption on a single free nucleon leading to an on-shell nucleon is forbidden by the laws of conservation of energy and momentum. Furthermore, the process as measured at meson facilities such as The Swiss Institute for Nuclear Research (SIN), the Clinton P. Anderson Meson Physics Facility, (LAMPF), and TRIUMF requires a momentum transfer greater than about 2 fm^{-1} that corresponds to rather small distances between nucleons. See, for example, the recent review by Ashery and Schiffer.¹

The best studied (both experimentally and theoretically) of these absorption reactions is $\pi^+ d \rightarrow pp$ at pion energies in the vicinity of the (3,3) resonance. In that case a conventional approach employing the diagrams of Fig. 1(a) and higher order terms, e.g., Fig. 1(b) works reasonably well.² This is because the pionic coupling to the (3,3) resonance is strong enough to mask the uncertainties in treating the exchanged virtual meson.

The different process of π^- absorption on a pair of bound protons may not occur through the conventional nuclear dynamical process and, therefore, may be a reasonable candidate to have a quark model description. The cross section for this process may be determined from π^- absorption on ${}^3\text{He}$ by measuring an outgoing proton and neutron in coincidence.^{3,4} As indicated in Fig. 1(c), the conservation of angular momentum, parity, and isospin forbids the formation of an intermediate ΔN state by the absorption of a p -wave pion. The initial pp system is mainly in a 1S_0 state with isospin $T=1$. Thus the total angular momentum and parity is $J^\pi=1^+$, if the pion is in a p -wave. Then the final pn state can have quantum numbers 3S_1 or 3D_1 , so $T=0$. The ΔN state can have only $T=1$ or 2, so the formation of an inter-

mediate ΔN state is not allowed. (In the π^+ absorption reaction the isospin of the initial state is $T=1$. Since the usually dominant term is very much suppressed,³⁻⁶ one may be free to search for more exotic explanations).

Let us begin with a review of previous calculations. These are based on the standard meson-baryon approach. Several authors have asserted that these computations supply terms that are too small to explain π^- absorption on a bound pair of protons. The statement seems to be correct, if one treats each theoretical idea separately. For example, Moinester *et al.*⁴ show that the cross sections computed by Toki and Sarafian⁵ are too small, but only by about a factor of 2.

Lee and Ohta,⁶ apparently using the same basic dynamics [Fig. 1(a)] and including higher order effects [e.g., Fig. 1(b)] absent in Ref. 5 obtained very small cross sections. The difference with Ref. 5 arises from the influence of the crossed-pion diagram of Fig. 1(d), included by Toki and Sarafian, but absent in Ref. 6. The intermediate state has two pions, so the selection rule suppression seen in connection with Fig. 1(c) does not apply. The importance of terms like Fig. 1(d) has been raised in connection with the related continuum reaction $pn \rightarrow pp\pi^-$ by Hwang and Cao.⁷

Another possibility is to include the influence of nucleon excitations⁸ as in Fig. 1(e). As shown in Ref. 8, this mechanism also leads to almost half of the cross section. The angular distribution is flatter than the data.

The recent work of Maxwell and Cheung⁹ must also be mentioned. These authors include terms with intermediate nucleon states, as e.g., in Fig. 1(f) and obtain cross sections for pion absorption on the pp pair that are very much larger than measured ones. This could be because some nucleon-nucleon final state interactions are neglected, and the pion-nucleon vertex function is treated in a static approximation.

Given the current uncertainty in applying the conventional meson-baryon picture to the $\pi^- + pp \rightarrow pn$ reaction, it seems reasonable to study how quark interactions can be used to calculate the cross section. That is the purpose of this paper. A model^{10,11} in which one uses baryonic (NN, ΔN , etc.) degrees of freedom for large separations (r greater than a parameter r_0) and six-quark bags to represent the short distance ($r < r_0$) wave func-

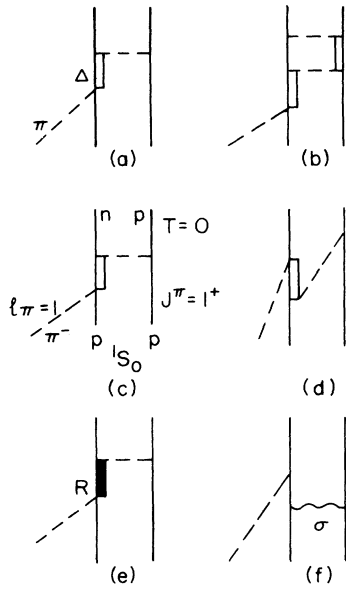


FIG. 1. Conventional mechanisms for π absorption reactions.

tion is employed at energies below that of the (3,3) resonance. Only the short distance quark contributions are included here, even though a careful calculation including all of the different conventional mechanisms of Fig. 1 might reproduce the essential features of the data. The motivation is that, for pion absorption, the biggest contributions of the terms of Fig. 1 occur for small distances between the baryons. But it is those very same contributions that are eliminated and replaced by quark contributions, if one employs the quark-baryon hybrid approach of Refs. 10–13. Thus it may be that a complete calculation would lead to quark dominance of this process. For this reason it is appropriate to compare our quark-only results with data at this early stage. Furthermore, as discussed above, there is a large diversity of opinion^{5–9} regarding the selection of the most important conventional mechanisms. In any case, it should be clear that a thorough understanding of the absorption process can only come about from a more complete investigation than is presented here. Polarization measurements will also be required.¹⁴

It is necessary to mention some of the limitations and restrictions of the present calculation. First, only s and p wave pions are included. Hence the present work is limited to energies below the (3,3) resonance, where d -wave effects are expected to be small.⁵ It is also true that our numerical results are sensitive to the nucleon-nucleon potential employed to compute six-quark probabilities, and to the choice of nucleon-nucleon phase shifts, see below. Other causes for concern are the use of the nonrelativistic quark model, and that the magnitudes of the predicted total cross sections depend strongly on r_0 . The results are that quark effects can account for a substantial fraction of the observed total cross sections and qualitatively reproduce the shape of the angular distributions. The present results and conclusions

update those of a preliminary report.¹⁰

The outline of the remainder of this paper is as follows. The salient features of the model^{10–13} are discussed briefly in Sec. II. This model is applied to the computation of the quark contributions to the amplitude for the π -pp absorption process in Sec. III. That section also includes formulae for the angular distributions and polarization observables. Comparison with data and predictions are presented in Sec. IV. Section V is reserved for a few summary remarks.

II. BUILDING THE NUCLEUS FROM NUCLEONS, MESONS, AND SIX-QUARK BAGS

We examine those nuclear reactions and properties that are *not* due to the influence of single nucleons. If a process requires two nucleons to be close together, the explicit quark degrees of freedom might be important. To concentrate on such quark aspects, it is worthwhile to consider many different processes, since a single reaction would not be expected to provide definitive information. Thus one needs a versatile procedure. Furthermore, it is desirable to employ an approach that avoids the difficulties of constructing the individual nucleons and their motion in the nuclear shell model potential completely from quantum chromodynamics (QCD).

We start with the idea that the conventional baryon-meson treatment is a good description of the long range aspects. In particular, consider two nucleons bound in a nucleus. At large separations one employs $\psi_{NN}(\mathbf{r})$, the conventional nucleon-nucleon wave function. Here r is the distance between the nucleons, which are treated as having no size. How might the composite nature of the nucleon modify ψ_{NN} ? Here we apply standard coupled channel methods. Suppose that the nucleons are sizable objects of three quarks. At large separations the nucleons do not touch and quarks and gluons are not exchanged. Next, imagine that the nucleons overlap. In that case, effects such as gluon exchanges and the influence of the quark-quark Pauli principle enter. If the volume of the overlapping region is small, one may expect that the system mainly consists of two nucleons, but with a modified wave function, $\tilde{\psi}_{NN}$ ($=\psi_{NN}$ for large r). But when the nucleons are very close, states that are *not* products of two nucleon internal wave functions may be formed. In that case, there is another component of the full wave function, that is orthogonal to $\tilde{\psi}_{NN}$. Call this new piece the six-quark wave function Φ_{6q} . Then one may write

$$\Psi = \tilde{\psi}_{NN} + \Phi_{6q} . \quad (1)$$

One way to ensure that $\tilde{\psi}_{NN}$ and Φ_{6q} are orthogonal is to let Φ_{6q} also be a color-singlet product of two three-quark objects, each of which carries color. With this definition, Eq. (1) is a useful separation, because operators that do not depend on color, such as those used in photon or pion absorption, have no matrix elements that connect the two components. (The nucleon cannot be converted to a nonsinglet color component by an operator containing no color.) Thus many interference effects are eliminated.

Confinement requires that it takes an infinite amount of energy to separate two “baryons” with opposite color. Then Φ_{6q} is concentrated near the origin. The picture of Ψ consisting of an ordinary component and a “hidden color” component is qualitatively similar to the resonating group method (RGM) results of Oka and Yakazi¹⁵ for the deuteron. Furthermore, Yamauchi and Wakamatsu¹⁶ have presented a detailed calculation showing that the separation used in Eq. (1) is a well-defined result of an RGM calculation. The use of the separation of Eq. (1) is neither necessary or unique.¹⁷ Nonetheless, it is well defined and has numerous phenomenological advantages.

The next step is to discuss Φ_{6q} . Computing this wave function from QCD is very difficult, so we settle for imposing some reasonable constraints. First, take Φ_{6q} to consist of six antisymmetrized quarks in a single spherical bag centered at $r=0$. The spatial wave function is taken to be symmetric: the [6] symmetry if Young diagrams are employed. The [6] symmetry has only a 10% probability of being a two-nucleon product state, so using it is an easy way to implement the orthogonality between $\tilde{\psi}_{NN}$ and Φ_{6q} in an approximate yet reasonably accurate fashion.

Wave functions of arbitrary angular momentum having the [6] symmetry may easily be constructed; see Sec. III. This allows one to implement the necessary constraint that the wave function Φ_{6q} has the same angular momentum, parity, and isospin as the original nucleon-nucleon wave function.

The next step is to use probability conservation to restrict the overall strength of Φ_{6q} . In our picture the conventional wave function ψ_{NN} is replaced by a smaller one, $\tilde{\psi}_{NN}$, when quarks are included. Thus the probability in the NN channel has been decreased. We assume that the missing probability goes solely into the six-quark component and write

$$\int |\psi_{NN}|^2 d^3r - \int |\tilde{\psi}_{NN}|^2 d^3r \equiv P_{6q}, \quad (2)$$

where

$$P_{6q} = \int |\Phi_{6q}|^2 dV. \quad (3)$$

The volume element dV is an integral over the positions of all of the quarks.

The simplest method to get an estimate of P_{6q} is to assume that $\tilde{\psi}_{NN}(\mathbf{r}) = \psi_{NN}(\mathbf{r})$ at large distances. Then integrate in from large r to small r , using the presumably well-known nucleon-nucleon interaction, and stop at a separation r_0 where the conventional dynamics are expected to break down. If $r < r_0$, set $\tilde{\psi}_{NN}$ to zero. This corresponds to using a sharp cutoff on $\tilde{\psi}_{NN}$ so that

$$\tilde{\psi}_{NN}(r) = \theta(r - r_0) \psi_{NN}(r) \quad (4a)$$

and

$$P_{6q} = \int d^3r \theta(r_0 - r) |\psi_{NN}|^2. \quad (4b)$$

In this case the entire NN probability that would have been at $r < r_0$ is given over to the quarks. Another procedure for determining P_{6q} is discussed in Ref. 10. It is

evident that P_{6q} depends strongly on the value of r_0 . The consequences of this are discussed below. Since r_0 is an important parameter, it is necessary to examine its expected range of values. As discussed in Ref. 10, a range $0.7 \text{ fm} < r_0 < 1.2 \text{ fm}$ seems to be reasonable.

Two distances are needed to describe Φ_{6q} in our treatment. One is the value of r_0 which is the NN separation at which quark effects enter. But another parameter is needed to characterize the volume of the six-quark system. This is the radius of the six-quark bag, R_6 . (In a more complete theory R_6 and r_0 would have a definite relationship.) However, there are several arguments¹⁰ that indicate $R_6 > R_3$. In any case, the results of the calculation presented here are not sensitive to the value of R_6 .

III. PION ABSORPTION BY A SIX-QUARK BAG

Quark effects may be included via the process shown in Fig. 2. A π^- is absorbed by any of the u quarks in the six-quark bag. Models of systems of confined quarks must include π -quark (π - q) interactions if the requirements of chiral symmetry are to be met.^{12,18} Furthermore, the value of the π - q coupling constant is constrained by the observed value of the π -nucleon coupling constant.

The next step is to describe the calculations of the transition matrix elements and the observables. A brief overview is given first. This is followed by a more detailed discussion.

A. Overview

The initial pion has orbital angular momentum $l_\pi = 0$ or 1. The six-quark target state has the quantum number 1S_0 so that the quantum numbers possible for the final proton-neutron (pn) state are 3S_1 , 3P_0 , 3D_1 . Note that each component has $S = 1$. This feature arises from the pseudoscalarity of the pion and the 1S_0 nature of the pp state.

To proceed one computes the matrix elements of the pion-quark interaction Hamiltonian, $H_{\pi q}$, between the initial and final states. Thus, the various six-quark wave functions, their probabilities, and $H_{\pi q}$ must be specified. For this calculation it is important to use quark states of good J^π . Furthermore, the final proton and neutron are in a scattering state, so it is vital to be able to separate

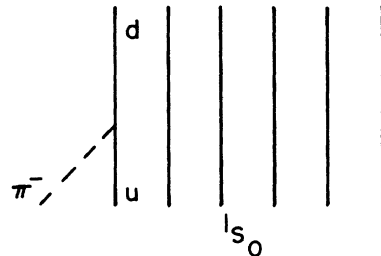


FIG. 2. Pion absorption by a six-quark bag.

the center of mass variable from the internal coordinates of the quarks. The easiest way to fulfill these requirements is to use the nonrelativistic quark model (NRQM) to treat the quark dynamics. The harmonic oscillator potential is employed, so standard techniques¹⁹ are used to obtain the correct internal quark position (ξ_i) and momentum operators.

The initial six-quark wave function $|^1S_0\rangle_{6q}$ is then a product of Gaussians involving $\sum_i \xi_i^2$ times a spin-isospin wave function that sets the quantum numbers to $T=1$, 1S_0 while ensuring a color singlet six-quark configuration. The final 3S_1 state is constructed in the same manner, but with $S \leftrightarrow T$. The final six-quark 3P_0

state is generated from the equation

$$|^3P_0\rangle_{6q} = \frac{1}{\sqrt{\mathcal{N}_p}} \sum_{i=1}^6 \sigma_i \cdot \mathbf{r}_i |^1S_0\rangle_{6q}, \quad (5)$$

where \mathcal{N}_p is a normalization constant that sets ${}_{6q}\langle ^3P_0 | ^3P_0 \rangle_{6q}$ to unity. One may think of the 3P_0 state as arising from promoting any of the six quarks from an S -state harmonic oscillator wave function to a P -state wave function, without affecting their center of mass. The 3D_1 state is obtained by using a tensor operator acting on the six-quark 3S_1 state:²⁰

$$|^3D_{1M_J}\rangle_{6q} = \frac{1}{\mathcal{N}_D} \sum_{i \neq j, M} \langle 2M 1M_S | 1M_J \rangle r_{ij}^2 Y_{2M}(\hat{\mathbf{r}}_{ij}) |^3S_{1M_S}\rangle_{6q}. \quad (6)$$

Important D -state contributions also arise from $^3S_1 - ^3D_1$ mixing via the pn tensor force acting at large separations.

The probability for the two bound protons to be closer than r_0 (set equal to P_{6q} here) can be obtained directly^{13,21} from elastic electron scattering data (for values of r_0 that are not too small²¹). The main assumption is that the three-nucleon spatial wave function is symmetric. The result is

$$P_{6q} = \frac{2}{\pi} r_0^2 \int_0^\infty q dq j_1(qr_0) F_{pt}(\sqrt{3}q), \quad (7)$$

where F_{pt} is the ratio of the nuclear to nucleon charge form factors.

The six-quark ‘‘probabilities’’ for the scattering states are defined explicitly below. It is sufficient here to state that these are obtained from pn scattering wave functions using recent potentials^{22,23} constrained by phase shifts and mixing parameters at the experimentally relevant pn kinetic laboratory energies (~ 425 MeV). The Bonn potential we use is an older version of the coordinate space one boson exchange potential (OBER) (R. Machleidt, private communication) which gives a better description of the pn system at $E_{\text{lab}} \approx 425$ MeV. The parameters of this potential differ only slightly from the published version and are presented in Table I.

TABLE I. Meson parameters used in the Bonn coordinate space (OBER) potential.

	$(g_\alpha^2/4\pi)(f_\alpha/g_\alpha)$	m_α (MeV)	Λ_α (MeV)
π	14.6	138.03	1300
η	3	548.8	1500
σ	8.0568	550	1750
δ	3.7064	983	1500
ω	20	782.6	1500
ρ	0.95 (6.1)	769	1300

The final point in this overview is the form of $H_{\pi q}$. Since nonrelativistic quark wave functions are employed we must use a nonrelativistic version of the usual relativistic or pseudovector coupling. Since our use of the NRQM is motivated by the desire to maintain Galilean invariance, we use the so-called Galilei invariant (GI) form^{24,25} of the π -quark vertex function; see below. This is a reasonable treatment provided the ratio of lower to upper components of the quark’s 4-spinors is similar to that of free quarks. In the NRQM [and the (MIT) bag model] the quarks are treated essentially as free particles at short distances. Thus using the GI form should be an adequate starting point. However, no proof has been presented here, and it seems that this issue requires further study. We shall see below that including the term proportional to the quark’s momentum is an important feature in obtaining a trend of the anisotropy for the observed angular distribution. In addition, lowest order relativistic corrections are known to improve the computed properties of NRQM wave functions.²⁶

B. Details of the calculation

The transition matrix element T_{fi} for the $\pi^-(pp) \rightarrow pn$ process is defined as

$$T_{fi} = \langle \psi_f | H_{\pi q} | \psi_i \rangle. \quad (8)$$

To continue, each of the three quantities on the right-hand side must be specified.

Only the quark contributions are included here, so $|\psi_i\rangle$ and $|\psi_f\rangle$ refer to the six-quark bag components of the initial bound pp wave function and final pn scattering wave function with incoming wave boundary conditions. Thus,

$$|\psi_i\rangle = |^1S_0\rangle_{6q} \sqrt{P_{6q}}, \quad (9)$$

where $|^1S_0\rangle_{6q}$ is the spatially symmetric six-quark configuration of spin zero and unit isospin. It is normalized to unity. The six-quark probability is defined in Eq. (7).

The final pn state is a bit more complicated since one

must include the different partial waves and maintain the requirements of rotational invariance. The simplest way to proceed is to start with the partial wave decomposition²⁷ of the standard pn wave function:

$$\langle \mathbf{r} | \text{pn}, \nu \hat{\mathbf{p}} \rangle = 4\pi \sum_{LL'JM'} i^{L'} \mathcal{Y}_{L'JM'}(\hat{\mathbf{r}}) \times Y_{LM'}^*(\hat{\mathbf{p}}) \psi_{L'JL}(r) \langle LM'1\nu | JM \rangle, \quad (10)$$

where only the required $S=1$ terms are shown. The quantities ν and $\hat{\mathbf{p}}$ are the third component of the Pauli spin and the unit vector in the direction of the pn relative momentum (proton minus neutron momentum).

Since we take $l_\pi=0,1$ only three final-state partial waves are possible, and it is worthwhile to list these explicitly. The different channels are designated by a, b, c . The corresponding pn channel wave functions²⁷ are $\phi_{a,b,c}$,

$$\phi_a = \frac{e^{i\delta_a}}{pr} (u_\alpha \mathcal{Y}_{011M} - w_\alpha \mathcal{Y}_{211M}), \quad (11a)$$

$$\phi_b = i \frac{e^{i\delta_b}}{pr} u_b \mathcal{Y}_{1100}, \quad (11b)$$

$$\phi_c = \frac{e^{i\delta_\beta}}{pr} (u_\beta \mathcal{Y}_{011M} - w_\beta \mathcal{Y}_{211M}), \quad (11c)$$

satisfying asymptotically ($r \rightarrow \infty$)

$$u_\alpha(r) \rightarrow \cos \epsilon \sin(pr + \delta_\alpha), \quad (12a)$$

$$w_\alpha(r) \rightarrow -\sin \epsilon \sin(pr - \pi + \delta_\alpha),$$

$$u_\beta(r) \rightarrow -\sin \epsilon \sin(pr + \delta_\beta), \quad (12b)$$

$$w_\beta(r) \rightarrow \cos \epsilon \sin(pr - \pi + \delta_\beta),$$

$$u_b(r) \rightarrow \sin(pr - \pi/2 + \delta_b), \quad (12c)$$

where δ_b is the 3P_0 phase shift, ϵ is the mixing parameter for $J^\pi=1^+$, and $\delta_\alpha, \delta_\beta$ are the eigen-phase-shifts.²⁸ For a real pn potential, the radial wave functions $u_{\alpha,\beta}$, $w_{\alpha,\beta}$, and u_b are all real.

The six-quark probabilities are defined above as re-

placing short-distance probability in the pn sector by an equal amount in the six-quark sector. Then the different probabilities are given by

$$P_{\alpha,\beta}(u) = \frac{1}{p^2} \int_0^{r_0} dr u_{\alpha,\beta}^2(r), \quad (13a)$$

$$P_{\alpha,\beta}(w) = \frac{1}{p^2} \int_0^{r_0} dr w_{\alpha,\beta}^2(r), \quad (13b)$$

$$P_b = \frac{1}{p^2} \int_0^{r_0} dr u_b^2(r), \quad (13c)$$

for the real pn forces used here. Using these definitions one may write the six-quark wave functions corresponding to the channel wave functions (11) for the final state as

$$|a\rangle = e^{i\delta_\alpha} [\sqrt{P_\alpha(u)} |{}^3S_{1M}\rangle_{6q} - \sqrt{P_\alpha(w)} |{}^3D_{1M}\rangle_{6q}], \quad (14a)$$

$$|b\rangle = i e^{i\delta_b} \sqrt{P_b} |{}^3P_0\rangle_{6q}, \quad (14b)$$

$$|c\rangle = e^{i\delta_\beta} [\sqrt{P_\beta(u)} |{}^3S_{1M}\rangle_{6q} - \sqrt{P_\beta(w)} |{}^3D_{1M}\rangle_{6q}]. \quad (14c)$$

The various six-quark wave functions are defined above in Eqs. (5) and (6) of Sec. III A. In using only two separate six-quark states $|{}^3S_{1M}\rangle_{6q}$ and $|{}^3D_{1M}\rangle_{6q}$, mixed as prescribed in (14a) and (14c), we ignore the effects of the quark-quark tensor force, which is considered insignificant.¹⁵ Thus, the tensor mixing displayed in Eqs. (14) arises from the pn tensor forces at distances greater than r_0 .

The values of the six-quark probabilities at lab energy 425 MeV, calculated via Eq. (13) for the coordinate space Bonn OBER,²³ are shown in Table II (Ref. 29) for values of r_0 in the range 0.6–1.1 fm. For a given value of r_0 , the largest six-quark probability is $P_\alpha(u)$, as expected, and the next in magnitude is $P_\beta(u)$ (both relating to 3S_1 components) as long as $r_0 < 1$ fm; for $r_0 > 1$ fm, the 3P_0 six-quark probability P_b is the second in magnitude. The 3D_1 probabilities $P_\alpha(w)$ and $P_\beta(w)$ remain relatively small. Note that Table II gives probabilities, but to compute angular distributions amplitudes are required. Thus the question of phases comes up. We are

TABLE II. Six-quark probabilities from the Bonn OBER at a lab energy of 425 MeV. P_{6q} in fm^3 and r_0 in fm.

r_0	$P_\alpha(u)$	$P_\alpha(w)$	$P_\beta(u)$	$P_\beta(w)$	P_b^b
0.60	0.0052	1.19×10^{-4}	1.85×10^{-3}	1.13×10^{-6}	3.14×10^{-4}
0.65	0.0075	2.19×10^{-4}	2.65×10^{-3}	3.49×10^{-6}	5.70×10^{-4}
0.70	0.0103	3.77×10^{-4}	3.65×10^{-3}	9.50×10^{-6}	9.86×10^{-4}
0.75	0.0137	6.13×10^{-4}	4.90×10^{-3}	2.34×10^{-5}	1.64×10^{-3}
0.80	0.0177	9.45×10^{-4}	6.34×10^{-3}	5.27×10^{-5}	2.62×10^{-3}
0.85	0.0221	1.39×10^{-3}	8.02×10^{-3}	1.09×10^{-4}	5.43×10^{-3}
0.90	0.0269	1.96×10^{-3}	9.86×10^{-3}	2.14×10^{-4}	6.02×10^{-3}
0.95	0.0319	2.65×10^{-3}	0.0118	3.92×10^{-4}	8.67×10^{-3}
1.00	0.0368	3.49×10^{-3}	0.0139	6.83×10^{-4}	0.0121
1.05	0.0416	4.45×10^{-3}	0.0159	1.13×10^{-3}	0.0164
1.10	0.0459	5.50×10^{-3}	0.0180	1.80×10^{-3}	0.0217

guided by Eq. (12) and take therefore $\sqrt{P_\alpha(u)}$ [$\sqrt{P_\beta(u)}$] to be positive (negative). [$\sqrt{P_{\alpha,\beta}(w)}$ is positive.] Thus the phases of the six-quark wave function are determined by those of exterior wave functions at $r=r_0$. This seems to be consistent with existing NRQM calculations.^{15,16}

To compute T_{fi} of Eq. (8) we need only specify $H_{\pi q}$. We write

$$H_{\pi q} = \frac{3}{5} \sqrt{4\pi} \frac{f}{m_\pi} \sum_{i=1}^6 \tau_i^{-1} \sigma_i \cdot \left[\mathbf{k} - \frac{\omega}{2m_q} (\vec{P}_i + \tilde{P}_i) \right] e^{i\mathbf{k} \cdot \mathbf{r}_i}, \quad (15)$$

where \mathbf{k} is the pion momentum in the π^-pp center of mass frame and $\omega = (k^2 + m_\pi^2)^{1/2}$. The indices i designate quark numbers, with \vec{P}_i (\tilde{P}_i) the i th quark momentum operator acting to the right (left), and τ_i^{-1} —the isospin lowering operator for quark i —defined by $\tau^{-1} = (\tau_x - i\tau_y)/\sqrt{2}$ in terms of the Pauli isospin matrices. The factor 3/5 is included so that the πNN coupling constant ($f^2 = 0.080$) is reproduced in the NRQM. The quark mass m_q is 338 MeV.

The computation of T_{fi} is now completely specified. First, use the partial wave sum (10) with the appropriate channel wave functions of Eq. (11) replacing $i^{L'} \mathcal{Y}_{L'JM}(\hat{\mathbf{r}}) \psi_{L'JL}(r)$ to obtain the six-quark final state in terms of the six-quark channel wave functions of Eq. (14). Then compute the matrix elements of $H_{\pi q}$ between the initial six-quark state $|^1S_0\rangle_{6q}$ and the different channel wave functions (14). The dynamics and matrix elements are essentially the same as in an earlier double charge exchange calculation.³⁰

The observables are obtained using standard techniques, so only the results are presented here. There are three partial-wave T 's, $T_{a,b,c}$, corresponding to the final 3S_1 , 3P_0 , 3D_1 pn scattering states, respectively. These are given by

$$T_a = (e^{i\delta_\alpha} \cos \epsilon A' - e^{i\delta_\beta} \sin \epsilon C') \sqrt{P_{6q}}, \quad (16a)$$

$$T_b = e^{i\delta_b} \sqrt{P_b} B \sqrt{P_{6q}}, \quad (16b)$$

$$T_c = (e^{i\delta_\alpha} \sin \epsilon A' - e^{i\delta_\beta} \cos \epsilon C') \sqrt{P_{6q}}, \quad (16c)$$

where

$$A' = \sqrt{P_\alpha(u)} A - \sqrt{P_\alpha(w)} C, \quad (17a)$$

$$C' = \sqrt{P_\beta(u)} A - \sqrt{P_\beta(w)} C, \quad (17b)$$

and A, B, C are given by the following six-quark matrix elements:

$$AY_{1M}^*(\hat{\mathbf{k}}) = {}_{6q} \langle ^3S_{1M} | H_{\pi q} | ^1S_0 \rangle_{6q}, \quad (18a)$$

$$BY_{00}^*(\hat{\mathbf{k}}) = {}_{6q} \langle ^3P_0 | H_{\pi q} | ^1S_0 \rangle_{6q}, \quad (18b)$$

$$CY_{1M}^*(\hat{\mathbf{k}}) = {}_{6q} \langle ^3D_{1M} | H_{\pi q} | ^1S_0 \rangle_{6q}, \quad (18c)$$

where the initial state is $T=1$ and the final states have isospin $T = [1 - (-1)^L]/2$. A straightforward but tedious evaluation yields

$$A = -\frac{2}{\sqrt{3}} u(k), \quad (19a)$$

TABLE III. pn phase shifts and mixing parameter at 425 MeV (lab) used in this work (the BB convention is adopted); in deg.

	$\delta_b(^3P_0)$	δ_α	δ_β	$\epsilon(^3S_1 - ^3D_1)$
Reference 31	-20.0	-4	-28	19.4
Reference 32	-22.5	-3	-28	11.0

$$B = \frac{1}{5} kb \left[1 - \frac{18}{5} \frac{1}{k^2 b^2} \frac{\omega}{m_q} \right] u(k), \quad (19b)$$

$$C = -\frac{1}{9\sqrt{2}} (kb)^2 \left[1 - 6 \frac{1}{k^2 b^2} \frac{\omega}{m_q} \right] u(k), \quad (19c)$$

with

$$u(k) = \frac{4\pi f k}{m_\pi} \exp\left(-\frac{5}{24} b^2 k^2\right), \quad (20)$$

the Gaussian form factor arising from the single-quark harmonic oscillator wave functions with size parameter b ($b \simeq 0.7$ fm). The phase shifts and mixing parameter are obtained at a pn laboratory kinetic energy of 425 MeV. One can use a single set as the pion energy varies between 37 and 83 MeV, since the pn energy changes only by 46 MeV and the pn observables vary very slowly at ~ 425 MeV. The values are taken from Refs. 31 and 32 and are given in Table III. For the α, β states the Blatt-Biedenharn²⁸ convention is used. The main difference between the two parameter sets is in the tensor mixing parameter $\epsilon(1^+)$. In Sec. IV below we discuss the sensitivity of the pion absorption calculation to such a difference.

The cross section is obtained by squaring T_{fi} , summing over final spins (denoted below by an overbar), multiplying by the final phase space factor, and dividing by the incident flux. We find, for the center-of-mass (c.m.) angular distribution of the observed proton,

$$\frac{d\sigma}{d\Omega} \simeq \frac{1}{16\pi^2} \frac{pM}{k} \overline{|T_{fi}|^2}, \quad (21)$$

where M is the nucleon mass and

$$\begin{aligned} \overline{|T_{fi}|^2} = & [3(|T_a|^2 + |T_c|^2) + |T_b|^2] \\ & - 2\sqrt{3} \operatorname{Re}[T_b(T_a - \sqrt{2}T_c)^*] \cos\theta \\ & + 3[|T_c|^2 - 2\sqrt{2} \operatorname{Re}(T_a T_c^*)] (\frac{1}{2} \cos^2\theta - \frac{1}{2}), \end{aligned} \quad (22)$$

so the Legendre-polynomial coefficients, A_L , for the angular distribution

$$\frac{d\sigma}{d\Omega} = \sum A_L P_L(\cos\theta), \quad (23)$$

are given by

$$A_0 = \frac{1}{16\pi^2} \frac{pM}{k} [3(|T_a|^2 + |T_c|^2) + |T_b|^2], \quad (24a)$$

$$A_1 = -\frac{1}{16\pi^2} \frac{pM}{k} 2\sqrt{3} \operatorname{Re}[T_b(T_a - \sqrt{2}T_c)^*], \quad (24b)$$

$$A_2 = \frac{1}{16\pi^2} \frac{pM}{k} 3[|T_c|^2 - 2\sqrt{2} \operatorname{Re}(T_a T_c^*)]. \quad (24c)$$

One can also compute spin observables. The vector polarization $P(\theta)$ perpendicular to the reaction plane is defined as

$$P(\theta) = \left[\frac{d\sigma_+}{d\Omega} - \frac{d\sigma_-}{d\Omega} \right] / \frac{d\sigma}{d\Omega}, \quad (25)$$

where $d\sigma_{\pm}/d\Omega$ is the cross section for the emitted proton to have spin up or spin down along $\mathbf{k} \times \mathbf{p}$. It is a reasonably straightforward matter to obtain¹⁴

$$P(\theta) = \frac{2 \operatorname{Im}(fg^*) \sin\theta}{|f|^2 + |g|^2 + 2 \operatorname{Re}(fg^*) \cos\theta}, \quad (26)$$

where

$$\begin{aligned} f &= -\sqrt{2}T_b - 3\sqrt{3}T_c \cos\theta, \\ g &= \sqrt{6}T_a - \sqrt{3}T_c. \end{aligned} \quad (27)$$

This completes the discussion of the technical details. Next, we present the results.

IV. COMPARISONS WITH DATA AND PREDICTIONS

At this stage we are able to compare our model with observations. Angular distribution data⁴ are available at 63 and 83 MeV. An experiment at 37 MeV has been performed, but is not yet analyzed. Another energy, 120 MeV, is under consideration for a future experiment. Thus the calculation will span the range from about 37 to 120 MeV. The higher energy is small enough so that the effects of d -wave pions should not be too important.

A. Total cross sections

The first step is to determine whether it is reasonable to expect that quark effects provide amplitudes large enough to be relevant. To do this, start by considering the total σ_T or angle integrated cross sections, $\sigma_T = 4\pi A_0$. Results for pion lab kinetic energies between 35 and 120 MeV are shown in Fig. 3. The data are from Ref. 4. Indeed, the computed values are sizable. Note also that the magnitudes of the cross sections

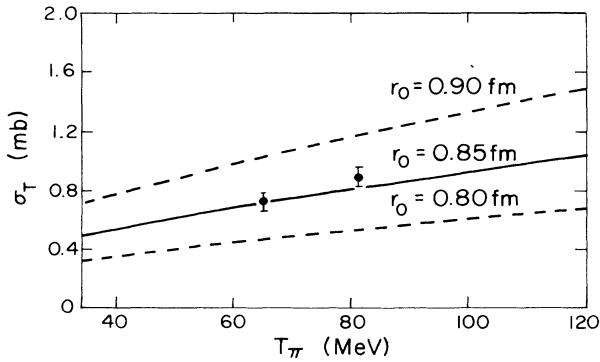


FIG. 3. Total cross sections as a function of energy and r_0 . Values of P_{6q} are taken from Ref. 13 and computed from Ref. 23.

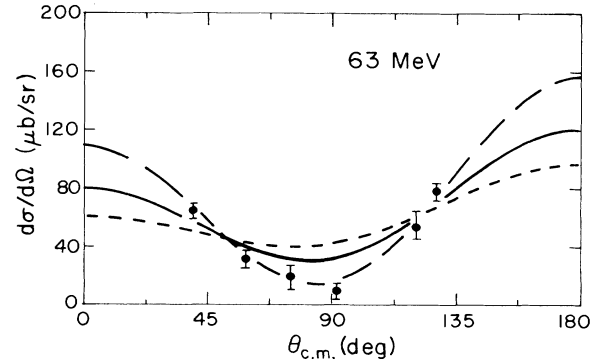


FIG. 4. Angular distribution at 63 MeV. Solid curve, phase shift set of Ref. 32; short-dashed curve, phase shift set of Ref. 31; long-dashed curve, $\delta_\alpha = \delta_\beta = \epsilon = 0$.

depend strongly on the value of r_0 . This is expected from the behavior of P_{6q} exhibited in Table I and in Ref. 13 (for the bound state). The results of Fig. 3 are independent of the phase shift set.^{31,32} The use of Lomon's potential²² gives also similar results, but r_0 must be greater than 1.05 fm since P_{6q} essentially vanishes otherwise.

One may be heartened by the result that the quark effects are not negligible, and that the model is able to reproduce the total cross section. On the other hand, the significant uncertainty in the magnitude of the computed total cross section shows that a more precise treatment of quark effects will ultimately be needed. The value $r_0 = 0.85$ fm leads to agreement with the data and is the only one used in the following computations.

B. Angular distributions

The next step is to consider the angular distributions. The data for energies around 63 MeV have had a strong impact since the work of Moinester *et al.*,⁴ and Fig. 4 shows the calculated distributions compared to observations. A first glance shows that qualitative agreement with the data is achieved. The general shape and char-

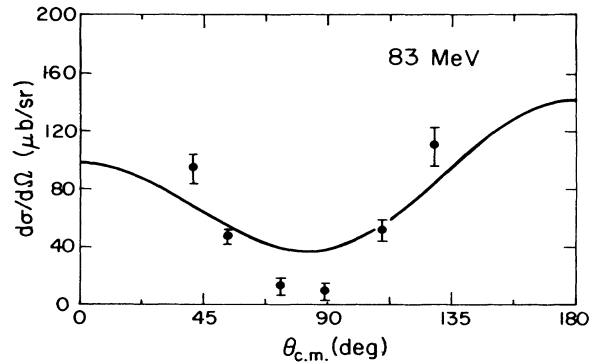


FIG. 5. Angular distribution at 83 MeV.

TABLE IV. Legendre coefficients of $d\sigma/d\Omega$. See Eqs. (23) and (24). A_L are given in $\mu\text{b}/\text{sr}$. (a) 63 Mev. (b) 83 MeV.

	Source	A_0	A_1	A_2
(a)	Aniol <i>et al.</i> ^a	55 ± 3	-45 ± 7	89 ± 7
	Arndt phase shifts ^b	55	-20	46
	Bugg phase shifts ^c	55	-18	24
(b)	Aniol <i>et al.</i> ^a	73 ± 5	-58 ± 9	123 ± 12
	Arndt phase shifts ^b	65	-22	54
	Bugg phase shifts ^c	65	-19	28

^aReference 4.

^bReference 32.

^cReference 31.

acter of the observations are reproduced using six-quark probabilities obtained with $r_0=0.85$ fm. The solid curve is obtained with the Arndt phase shifts³² and the short-dashed line is obtained with the phase shifts of Ref. 31. The computed angular distributions are mainly sensitive to the value of the 3S_1 - 3D_1 mixing parameter ϵ . For comparison, we present (long-dashed curve) an angular distribution with $\delta_\alpha=\delta_\beta=\epsilon=0$. This gives the best agreement. In the following we present and discuss only the results for the Arndt set; however, the above uncertainty should be kept in mind. If the Arndt phases are employed the salient features that the minimum occurs at an angle less than 90° and that the cross section is larger at 180° than in the forward direction are reproduced. These attributes are summarized by the computed values of $A_0=55$, $A_1=-20$, and $A_2=46 \mu\text{b}/\text{sr}$ [see Eqs. (23) and (24)] which are not too far from the experimental ones of Aniol *et al.*:⁴ $A_0=55 \pm 3$, $A_1=-45 \pm 7$, and $A_2=89 \pm 7 \mu\text{b}/\text{sr}$. The calculated magnitudes of A_1 and A_2 are a bit too small to obtain excellent agreement. Similar results are obtained for the angular distribution at 83 MeV as shown in Fig. 5. The coefficients of the Legendre expansion are summarized in Table IV.

The computed total cross sections depend very much on the value of r_0 , as noted in Fig. 3. However, the shape of the angular distribution is not at all sensitive to that parameter. Once the different curves are normalized to give the same result at 180° , there is no noticeable difference.

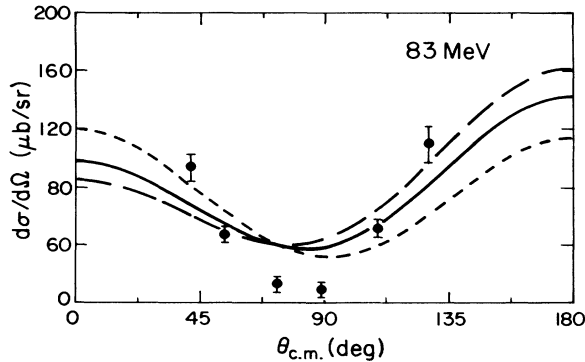


FIG. 6. Influence of the recoil term on $d\sigma/d\Omega$. Solid curve, with recoil; short-dashed curve, without recoil, $\omega \rightarrow 0$; long-dashed curve, ω/m_q is set to 1.

It is amusing to study the origin of the negative sign of A_1 . This term causes an asymmetry of the angular distribution about 90° and therefore indicates the presence of terms absent in the usually examined reaction $\pi^+d \rightarrow pp$. An examination of Eqs. (16b), (19b), and (24b) shows that the sign of A_1 is determined by the dominant recoil term proportional to ω . The influence of this recoil term is displayed in Fig. 6, in which the cross section obtained by neglecting the ω/m_q term of Eq. (15) is shown as a short-dashed line. In that case the angular distribution is essentially symmetric about 90° . It is reasonable to expect that including similar recoil terms (or using a more complete relativistic treatment) in conventional (baryon-meson) approaches will be important in reproducing the substantially negative value of A_1 that is observed experimentally. Note also that the form of the recoil term (proportional to the quark momentum) is model dependent. Equation (15) is derived in treatments which regard the pion as an elementary object. Another treatment, the 3P_0 model,³³ takes the pion to be a $q\bar{q}$ pair. The resulting pion-quark interaction can be expressed in the form of Eq. (15), but with ω/m_q replaced by unity.³³ The resulting angular distribution is the long-dashed curve of Fig. 6. The minimum occurs at an even more forward position and the fore-aft asymmetry is increased. (Thus using the 3P_0 model improves the agreement with the data if a slightly smaller value of r_0 is used.)

Incident pion kinetic energies of 37 and 120 MeV are

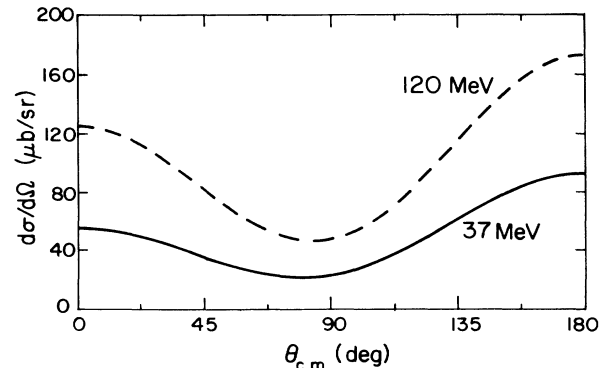


FIG. 7. Differential cross sections at 37 and 120 MeV.

of interest to ongoing and possible future experiments involving cross sections and polarizations.³⁴ The predicted angular distributions are shown in Fig. 7. Note that the (Arndt) NN phases of Table III appropriate for 63 MeV pions are used here.

V. SUMMARY

The application of the quark model of Refs. 10–13 to the calculation of observables for the $\pi^- + pp \rightarrow pn$ process leads to qualitative agreement with the trends of the data measured at pion kinetic energies of 63 and 83 MeV.

The correspondence of our model calculation with the data implies that quark effects may provide a substantial contribution to the complete amplitude. However, our explanation cannot yet be claimed to be unique or complete because of the various restrictions and limitations mentioned in the Introduction. The model may be ruled out by future measurements of angular distributions at other energies or by polarization measurements.

One interesting technical feature of the computation is

that the substantially negative value of A_1 (coefficient of asymmetry in the angular distribution) is obtained by including the term in the pion-quark interaction that depends on the quark momentum. This suggests that corresponding nucleon momentum terms should be included in conventional approaches if these are to reproduce the value of A_1 .

ACKNOWLEDGMENTS

We thank D. Ashery, M. A. Moinester, and E. Piasezky for initiating the interest of G.A.M., and subsequently of A.G., in this problem, and for numerous useful discussions and comments. We thank B.K. Jennings for useful discussions. Parts of the manuscript were put together while visiting LAMPF: G.A.M. (A.G.) would like to thank R. Boudrie (H.A. Thiessen) and the MP-10 (MP-14) group for their hospitality during Summer 1986 (1987). This work was supported in part by the U.S. Department of Energy and by the U.S.-Israel Binational Science Foundation, Jerusalem.

-
- ¹D. Ashery and J. P. Schiffer, *Annu. Rev. Nucl. Part. Sci.* **36**, 207 (1986).
- ²G. Jones, *Nucl. Phys.* **A416**, 157 (1984); D. F. Measday and G. A. Miller, *Annu. Rev. Nucl. Part. Sci.* **29**, 121 (1979); M. Betz *et al.*, in *Pion Production and Absorption in Nuclei*, AIP Conf. Proc. No. 79, edited by R. D. Bent (AIP, New York, 1982).
- ³D. Gotta *et al.*, *Phys. Lett.* **112B**, 129 (1982); G. Backenstoss *et al.*, *ibid.* **115B**, 445 (1982); D. Ashery *et al.*, *Phys. Rev. Lett.* **47**, 895 (1981); G. Backenstoss *et al.*, *Phys. Lett.* **137B**, 329 (1984).
- ⁴M. A. Moinester *et al.*, *Phys. Rev. Lett.* **52**, 1203 (1984); K. A. Aniol *et al.*, *Phys. Rev. C* **33**, 1714 (1986).
- ⁵H. Toki and H. Sarafian, *Phys. Lett.* **119B**, 285 (1982).
- ⁶T. S. H. Lee and K. Ohta, *Phys. Rev. Lett.* **49**, 1079 (1982).
- ⁷W.-Y. P. Hwang, private communication; Z. J. Cao, Ph.D. thesis, Indiana University, 1986; W.-Y. P. Hwang and Z. J. Cao (unpublished).
- ⁸R. S. Silbar and E. Piasezky, *Phys. Rev. C* **29**, 1116 (1984); **30**, 1365(E) (1984).
- ⁹O. V. Maxwell and C. Y. Cheung, *Nucl. Phys.* **A454**, 606 (1986).
- ¹⁰G. A. Miller, in *Workshop on Nuclear Chromodynamics*, edited by S. Brodsky and E. Moniz (World-Scientific, Singapore, 1986), p.343.
- ¹¹L. S. Kisslinger, *Phys. Lett.* **112B**, 307 (1982); E. M. Henley, L. S. Kisslinger, and G. A. Miller, *Phys. Rev. C* **28**, 1277 (1983).
- ¹²G. A. Miller, in *International Review of Nuclear Physics*, edited by W. Weise (World-Scientific, Singapore, 1984), Vol. 1, p. 189.
- ¹³V. Koch and G. A. Miller, *Phys. Rev. C* **31**, 602 (1985); **32**, 1106(E) (1985).
- ¹⁴E. Piasezky, D. Ashery, M. Moinester, G. A. Miller, and A. Gal, *Phys. Rev. Lett.* **57**, 2135 (1986).
- ¹⁵M. Oka and K. Yazaki, *Nucl. Phys.* **A402**, 477 (1983).
- ¹⁶Y. Yamauchi and M. Wakamatsu, *Nucl. Phys.* **A457**, 621 (1986).
- ¹⁷H. R. Petry, *Quarks and Nuclear Structure*, Vol. 197 of *Lecture Notes in Physics*, edited by K. Bleuler (Springer-Verlag, Berlin, 1983).
- ¹⁸A. W. Thomas, *Adv. Nucl. Phys.* **13**, 1 (1983); G. E. Brown and M. Rho, *Phys. Lett.* **82B**, 177 (1979).
- ¹⁹See, e.g., A. de Shalit and H. Feshbach, *Theoretical Nuclear Physics* (Wiley, New York, 1974), Chap. 4.
- ²⁰P. A. M. Guichon and G. A. Miller, *Phys. Lett.* **134B**, 15 (1983).
- ²¹J. L. Friar, *Nucl. Phys.* **A156**, 43 (1970), and private communication.
- ²²E. L. Lomon, *Phys. Rev. D* **26**, 576 (1982), and private communication.
- ²³R. Machleidt, K. Holinde, and Ch. Elster, *Phys. Rep.* **149**, 1 (1987); R. Machleidt, private communication.
- ²⁴See, e.g., D. S. Koltun and A. R. Reitan, *Phys. Rev.* **141**, 1413 (1966).
- ²⁵H. W. Ho. M. Alberg, and E. M. Henley, *Phys. Rev. C* **12**, 217 (1975).
- ²⁶See, e.g., C. Hayne and N. Isgur, *Phys. Rev. D* **25**, 1944 (1982).
- ²⁷M. L. Goldberger and K. M. Watson, *Collision Theory* (Wiley, New York, 1964).
- ²⁸J. M. Blatt and L. C. Biedenharn, *Phys. Rev.* **86**, 399 (1952).
- ²⁹We thank D. Driscoll for providing this table.
- ³⁰G. A. Miller, *Phys. Rev. Lett.* **53**, 2008 (1984).
- ³¹D. V. Bugg *et al.*, *Phys. Rev. C* **21**, 1004 (1980).
- ³²R. A. Arndt, *Phys. Rev. D* **28**, 97 (1983).
- ³³A. Le Yaouanc *et al.*, *Phys. Rev. D* **8**, 2223 (1973); **9**, 1415 (1974); **11**, 1272 (1975).
- ³⁴TRIUMF Proposal E460 (Spokesmen: P. Walden, D. Hutcheon, and M. Moinester).